NJC

PAPER

View Article Online
View Journal

Cite this: DOI: 10.1039/c4nj01443j

A novel water-soluble quantum dot–neutral red fluorescence resonance energy transfer probe for the selective detection of megestrol acetate†

Li-Yun Wang, Ling-Yu Dong, Luan Chen, Ya-Bing Fan, Jing Wu, Xiang-Feng Wang and Meng-Xia Xie*

Received (in Montpellier, France) 28th August 2014,
Accepted 28th October 2014

DOI: 10.1039/c4nj01443j

www.rsc.org/njc

A novel water-soluble beta-cyclodextrin (β-CD)-functionalized ZnS quantum dot (QD)–neutral red (NR) fluorescence resonance energy transfer (FRET) probe for the selective determination of the concentration of megestrol acetate in river water has been developed. The water-soluble and low-toxicity β-CD-functionalized ZnS QDs were first synthesized, and their characterization was confirmed by transmission electron microscopy and infrared, UV-vis and fluorescence emission spectra. The NR molecule can enter the cavity of the β-CD anchored onto the surfaces of the ZnS QDs in its neutral form, forming the FRET probe. Compared with other steroid hormones, the probe can selectively recognize megestrol acetate at a lower concentration level. The possible underlying mechanism of the probe with nine steroid hormones was discussed in detail. The fluorescence quenching fractions of the probe presented a satisfactory linearity with the concentrations of megestrol acetate, and its limit of detection was calculated to be 0.0083 μM. Coupled with sample pretreatment procedures, the probe has been applied to the determination of megestrol acetate in river water. The average recoveries of megestrol acetate in the spiking levels of 0.001 μM–10 μM ranged from 97% to 110% with a relative standard deviation below 15%, which was similar to those for HPLC or MS techniques.

1. Introduction

Quantum dots (QDs) are popular nanostructured materials that possess unique optical and electronic properties, such as size-dependent emission, high quantum yield and simultaneous resistance to photobleaching.[1–3] Thus, QDs have generated a great deal of attention over the past two decades and are recognized as a new type of prospective fluorescent probes that are useful for molecular recognition,[4] metal ion detection,[5,6] biological macromolecule interaction,[7,8] cell imaging,[9–11] and other applications. However, the practical applications of the QDs for the specific determination of target analytes are dependent on the modification of the QD surfaces.

Early research mainly focused on small organic molecules, primarily thiols, as the modification agents of the QD surfaces,[12–15] and in recent years, numerous functional groups or biological macromolecules have been successfully utilized.[16–20] For example, DNA or RNA fragments can act as the recognition reporters and are connected to the QD surface to form fluorescent probes for genetic target strand detection,[21] and the high specificity of hybridization between QD–DNA probes and the target strand with a complementary sequence forms the basis for the detection of DNA.[22]

Cyclodextrins (CDs) are cyclic oligosaccharides in α, β or γ forms, which can act as molecular hosts for forming inclusion complexes with various guest molecules due to their special molecular structure consisting of a hydrophobic internal cavity and a hydrophilic external surface. These CD-functionalized QD particles were successfully utilized to selectively and reversibly control the analyte-induced fluorescence change in the QDs.[23–27] Li and Han reported the synthesis of the water-soluble CdSe/ZnS QDs by a simple sonochemical method using α-, β- and γ-CDs as surface-modifiers, and the obtained probes have high sensitivity for the determination of *p*-nitrophenol and 1-naphthol.[23] They also reported that α-CD- or β-CD-functionalized CdSe/ZnS QDs are useful for the highly enantioselective fluorescent recognition of amino acids.[28] Furthermore, β-CD-functionalized CdSe/ZnS QDs have been used for the optical sensing of 1-adamantanecarboxylic acid and 4-hydroxytoluene and the chiroselective sensing of D,L-phenylalanine and D,L-tyrosine.[29] An optical biosensor for the determination of amantadine based on FRET between β-CD-functionalized CdTe QDs and rhodamine B has been constructed.[30] It has

Analytical & Testing Center of Beijing Normal University, Beijing 100875, P. R. China. E-mail: xiemx@bnu.edu.cn; Fax: +86-10-58800076; Tel: +86-10-58807981

† Electronic supplementary information (ESI) available. See DOI: 10.1039/c4nj01443j

also been found that the addition of ferrocene derivatives to the β-CD-anchored QD system would result in a significant decrease in the band-edge emission *via* a photoinduced electron transfer mechanism, while upon the addition of adamantine to the system, a high luminescence response can be observed.[31] Although the development of fluorescent probes based on the system has been impressive, the scientific community is still actively attempting to develop additional selective and sensitive approaches for practical applications.

FRET between donor and acceptor chromophores has been extensively utilized to explore the interaction mechanism between biomacromolecules and their ligands[32] and to develop novel approaches for the determination of target analytes.[33–36] Amine-modified QD605 and Cy5-labeled oligodeoxynucleotides were chosen as the FRET pair and were encapsulated in lipoplexes; upon excitation at 405 nm, the QD-FRET mediated Cy5 emission suggested compact and intact lipoplexes, and the disappearance of QD-FRET-mediated Cy5 emission indicated the dissociation of the lipoplexes.[37] Efficient FRET from molecular beacon-modified CdTe QDs to graphene oxide has also been reported, and the strong interaction between the single-stranded DNA of the molecular beacon loop structure and graphene oxide was combined to establish a novel selective and sensitive platform for the fluorescence-quenching detection of DNA.[38] Due to the sensitive and selective properties of the FRET-based systems for analyte determination purposes, the continued development of more pragmatic systems is the main branch of analytical chemistry.

Steroid hormones play an important role in maintaining life, immune regulation, skin diseases and birth control. These hormones may be released into the environment by illegal sewage effluent and can potentially interfere with the normal function of the endocrine system, which would affect both reproduction and development in wildlife.[39–41] Therefore, monitoring the residues of the steroid hormones in the environment is important. The conventional techniques for the analysis of steroid hormones are HPLC, GC–MS and LC–MS–MS.[40,42–44] However, some disadvantages of these approaches exist, such as the tedious nature of these procedures, the difficultly in performing the experiments and the high cost of equipment. Optical analysis is considered a more convenient and alternative technique due to its inherent simplicity and high sensitivity. Recently, there have been several reports of rapid detection methods for steroid hormones. For example, commercially available rapid ELISA kits were validated for the quantification of oestrogens in sewage effluent samples,[45] and a unique FRET-based aptasensor was constructed for the determination of 17 beta-estradiol using a quantum dot bioconjugate as a nano-biosensor and a fluorescence-labelled anti-17 beta-estradiol aptamer as a bio-recognition molecule.[46]

In this report, a β-CD-ZnS QD–NR FRET probe has been developed (see Scheme 1). Mono-6-thio-β-CD was prepared by a simple two-step synthesis and then conjugated with the ZnS QD particles (see Scheme 1A). The dye NR could bind to the cavity of β-CD, and the FRET process could occur between β-CD-functionalized ZnS QDs and NR (see Scheme 1B(i)). The developed β-CD-ZnS QD–NR FRET system was sensitive to steroid

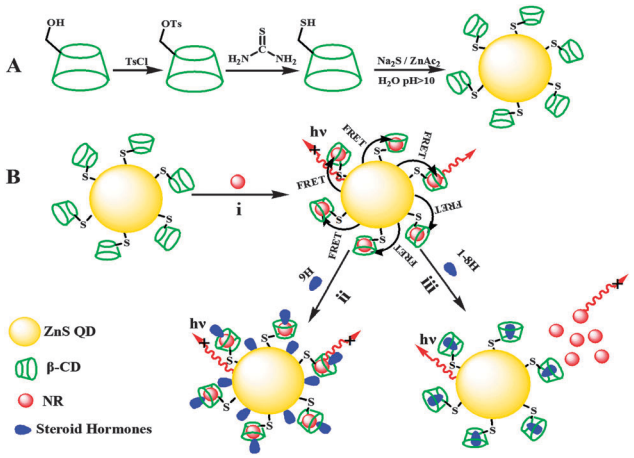

Scheme 1 (A) Schematic illustration for the preparation of the β-CD modified ZnS QDs. (B) Formation of the FRET system between β-CD-modified ZnS QDs and neutral red NR (i); the possible fluorescence quenching mechanism of the CD-QD–NR FRET fluorescence probe which was induced by 9H (ii); competitive assay of the other eight steroid hormones (1–8H) and NR on the cavities of the fluorescence probe (iii).

hormones (see Scheme 1B(ii) and (iii)). The conditions of the FRET system have been optimized, and the behaviours of the fluorescence quenching properties for the FRET system induced by various types of steroid hormones have been systematically investigated. An interaction mechanism of the FRET system with different steroid hormones has been proposed. Consequently, a simple, rapid and low-cost analytical method based on a FRET fluorescence probe for the determination of the concentration of megestrol acetate in river water samples has been developed.

2. Experimental methods

2.1. Chemicals and apparatus

All chemicals obtained from commercial suppliers were used without further purification. Zinc acetate dehydrate ($Zn(Ac)_2 \cdot 2H_2O$, 99.0%) and sodium sulphide nonahydrate ($Na_2S \cdot 9H_2O$, 98.0%) were obtained from Sinopharm Chemical Reagent Co., Ltd (Beijing, China). Neutral red (NR) and testosterone (98.0%) were purchased from Acros Organics (New Jersey, USA). Progesterone (98.0%) was obtained from Aladdin Chemistry Co., Ltd (Shanghai, China). 4-Androstene-3,17-dione(98.0%), stanozolol (98.0%) and 17α-hydroxyprogesterone (97.0%) were obtained from Dr Ehrenstorfer GmbH (Augsburg, Germany). Medroxyprogesterone acetate (96.0%) and megestrol acetate (96.0%) were obtained from TCI Chemicals (Shanghai, China). Estrone (96.0%) and 17-beta-estradiol (96.0%) were obtained from J&k Chemical. Ltd (Beijing, China). C18 (40–60 μm) was obtained from Merck (Darmstadt, Germany). Acetonitrile and hexane were of HPLC-reagent grade and were provided by Sinopharm Chemical Reagent Beijing Co., Ltd (Beijing, China), and other chemicals and reagents were of analytical grade and were obtained from Beijing Chemical Factory (Beijing, China). Ultrapure water was prepared using a Milli-Q water system

(18.3 MΩ cm^{-1}) from a Millipore purification system (Barnstead Corp., Boston, USA).

The SPE cartridge (6 mL) and sieve plates were purchased from Jiruisen (Beijing, China). Separation was carried out using solid-phase extraction equipment with 12-port vacuum manifolds (Supelco, Bellefonte, PA, USA). Concentration was performed using an EVA 30A nitrogen-blowing instrument (Polytech. Co. Ltd Beijing, China).

2.2. Preparation and characterization of the β-CD-functionalized ZnS QDs

The mono-6-thio-β-CD was prepared according to the procedures described previously.[26,47] Briefly, to a three-necked flask, $Zn(Ac)_2 \cdot 2H_2O$ (0.11 g, 0.5 mmol), mono-6-thio-β-CD (0.85 g, 0.75 mmol) and water (50 mL) were added, and the mixture solution was stirred until the components dissolved. The pH of the solution was adjusted to 11 using 1 M NaOH, and then the mixture was refluxed for 20 min after the removal of air by N_2 bubbling for 15 min at room temperature. Thereafter, 5 mL of $Na_2S \cdot 9H_2O$ (0.12 g, 0.5 mmol) was added to the solution, and the solution was stirred for 20 min under N_2 protection; the solution was then aged at room temperature for 6 h to form the β-CD-functionalized ZnS QDs. For purification, the obtained product was precipitated with ethanol three times and then separated by centrifugation and dried under vacuum. The prepared β-CD-functionalized ZnS QDs were refrigerated at 4 °C and were quite stable and water soluble. 3-Mercaptopropionic acid (MPA)-modified ZnS QDs were prepared using similar procedures.

For characterization, the infrared spectra of β-CD and β-CD-functionalized ZnS QDs were collected using a Nicolet Nexus 670 FT-IR spectrometer (Thermofisher, Madison, WI, USA) in the range of 4000–400 cm^{-1} with 64 scans at a resolution of 4 cm^{-1}. The morphology of the β-CD-functionalized ZnS QDs was characterized using a Tecnai F20 transmission electron microscope (FEI) operated at a voltage of 200 kV (Hillsboro, USA). UV-vis absorption spectra of β-CD-functionalized ZnS QDs and NR in a phosphate-buffered solution (pH 8.5) were acquired using a SPECORD 200 spectrophotometer (analytikjena, Gena, Germany) in the range of 220–700 nm with a slit of 2 nm. Fluorescence emission spectra of β-CD-functionalized ZnS QDs and NR in a phosphate-buffered solution (pH 8.5) were obtained using a HORIBA Jobin Yvon FluoroMax-4 fluorometer (JY, Paris, France) over ranges of 350–550 nm and 500–700 nm at an excitation wavelength of 300 nm. The slit width for both excitation and emission was 5 nm.

The quantum yield of the β-CD-functionalized ZnS QD particles was directly determined in ultrapure water using a HORIBA Jobin Yvon FluoroMax-4 fluorometer with a F-3029 Integrating Sphere accessory (JY, Paris, France).

2.3. Preparation of stock solution

The phosphate buffer solution (10 mmol L^{-1}) was adjusted to pH 2.5, 4.5, 6.5, 8.5 and 10.5 using NaOH or H_3PO_4. β-CD-functionalized ZnS QDs were dissolved in ultrapure water to prepare stock solutions with a concentration of 0.01 mol L^{-1} (estimated according to ZnS molecules). β-CD was dissolved in ultrapure water to prepare a stock solution with a concentration of 0.01 mol L^{-1}. NR was dissolved in ultrapure water to prepare a stock solution with a concentration of 3.5×10^{-3} mol L^{-1}. Nine types of steroid hormones were dissolved in ethanol to prepare stock solutions with a concentration of 4.0×10^{-3} mol L^{-1}.

2.4. Fluorescence emission spectra

To study the pH effect on the FRET system, the mixed solution of β-CD-functionalized ZnS QDs and NR was diluted with buffer solutions at different pH values (pH 2.5, 4.5, 6.5, 8.5 and 10.5). The final concentrations of β-CD-functionalized ZnS QDs and NR were 300 μM and 1.8 μM, and the fluorescence spectra were collected.

To study the effect of the NR concentrations on the FRET system, a series of concentrations of NR (0, 0.2, 0.4, 0.6, 0.8, 1.0, 1.2, 1.4, 1.6, 1.8, 2.0, 2.2, and 2.4 μM) were mixed with β-CD-functionalized ZnS QDs (final concentration 300 μM) in a buffer solution (pH 8.5), and then the fluorescence spectra were collected.

To study the response of the β-CD-QD–NR FRET fluorescence probe to steroid hormones, the nine steroid hormones were mixed with the probe in a buffer solution (pH 8.5). The final concentrations of the β-CD-functionalized ZnS QDs and NR were 300 μM and 1.8 μM, respectively, and for the steroid hormones, the concentrations were 10 μM, 60 μM and 180 μM. Subsequently, their fluorescence spectra were collected.

To investigate the effects of coexisting ions on the β-CD-QD–NR FRET fluorescence probe, ten kinds of common ions (Ca^{2+}, Cd^{2+}, Mn^{2+}, Co^{2+}, Mg^{2+}, Na^{+}, K^{+}, Fe^{3+}, Fe^{2+} and Cu^{2+}) were mixed with the probe in buffer solution (pH 8.5), respectively. The final concentrations of β-CD-functionalized ZnS QDs and NR were 300 μM and 1.8 μM, individually, and the concentration for each ion was 180 μM, and then, their fluorescence spectra were collected.

The effect of concentration on the steroid hormone fluorescence emission intensities of the β-CD-QD–NR FRET fluorescence probe was determined as follows. The mixtures of megestrol acetate and the probe in buffer solutions (pH 8.5) with final concentrations of 0, 0.25, 0.5, 1.0, 5.0, 10, 20, 40 and 60 μM megestrol acetate were prepared, and their fluorescence spectra were collected. Similarly, the mixture solutions of the probe and various concentrations of the other steroid hormones (0, 60, 120, 180, 240, 300 and 360 μM) were prepared, and their spectra were individually collected.

The above-mentioned fluorescence emission spectra were collected using a 370 nm filter and scanned in the range of 380–700 nm at an excitation wavelength of 300 nm. The slit width for both excitation and emission was 5 nm.

Control experiments for the interaction of NR and steroid hormones were conducted *via* the following methodology. The NR solution was diluted to 1.8 μM with pH 8.5 buffer solution, and the mixture of NR and β-CD was diluted to concentrations of 1.8 μM and 300 μM with buffer solution (pH 8.5) Then, a series of mixture solutions (pH 8.5) of NR (1.8 μM) and β-CD (300 μM) and steroid hormones (megestrol acetate (60 μM) and other steroid hormones (180 μM)) were prepared. Their fluorescence spectra were recorded in the range of 500–700 nm at the excitation wavelength of 300 nm, and the slit width for excitation and emission was 5 nm.

Control experiments for the interaction of β-CD-functionalized ZnS QDs and steroid hormones followed the procedure outlined below. The β-CD-functionalized ZnS QDs were diluted to 300 μM with buffer solution (pH 8.5). The mixture solutions of β-CD-functionalized ZnS QDs (300 μM) and megestrol acetate (60 μM) and other steroid hormones (180 μM) were prepared. Their corresponding fluorescence spectra were collected in the range of 350–550 nm at an excitation wavelength of 300 nm.

2.5. Fluorescence lifetime measurements

The NR solution was diluted to 1.8 μM with buffer solution (pH 8.5). The mixture solutions of β-CD-functionalized ZnS QDs (300 μM) and NR (1.8 μM) were prepared with pH 8.5 buffer. A series of mixed solutions for β-CD-functionalized ZnS QDs (300 μM) and NR (1.8 μM) and the steroid hormones (60 μM for megestrol acetate and 180 μM for other steroid hormones) were prepared with buffer solution (pH 8.5). Fluorescence lifetime measurements were carried out by the time-correlated single-photon counting (TCSPC) method using a Horiba Jobin Yvon Fluorocube (JY, Paris, France).

2.6. Spiking recoveries of megestrol acetate in river water samples

River water samples were collected from local rivers in Beijing and filtered prior to analysis. Five spiking levels of megestrol acetate (0.001, 0.01, 0.1, 1.0 and 10 μM) were added to 320 mL of river water samples. Then, the spiked water samples were purified and enriched by solid-phase extraction (SPE) *via* the following procedure.[41,48,49]

The C18 (1.0 g) sorbents were used to fill a 6 mL SPE cartridge and then conditioned with 10 mL of *n*-hexane, 10 mL of acetonitrile and 10 mL of ultrapure water. Thereafter, the spiked water sample (320 mL) was loaded onto the SPE cartridge at a flow rate of 4–5 mL min^{-1}, and the cartridge was dried under vacuum. The SPE cartridge was eluted with 5 mL of acetonitrile, and the elution was evaporated using a gentle stream of nitrogen gas. The residues were dissolved with 0.1 mL of ethanol and 1 mL of buffer solution (pH 8.5), and the β-CD-QD–NR FRET fluorescence probe was added; then, the solution was diluted to 3.2 mL with buffer solution. Each sample was assayed five times (n = 5), and the corresponding fluorescence spectra were collected.

3. Results and discussion

3.1. Characterization of the β-CD-functionalized ZnS QDs

Scheme 1A gives details of the preparation and grafting of the mono-6-thio-β-CD onto the surface of ZnS QD particles. The obtained β-CD-functionalized ZnS QDs have been characterized by FTIR spectra, transmission electron microscopy, UV-vis absorption and fluorescence emission spectroscopic methods.

No typical absorption band was observed in the FTIR spectra of ZnS QDs from 4000 to 500 cm^{-1},[50–52] and the IR spectra of water-soluble ZnS QDs usually reflect the absorption bands of their modifier. Fig. 1A shows the transmission FTIR spectra

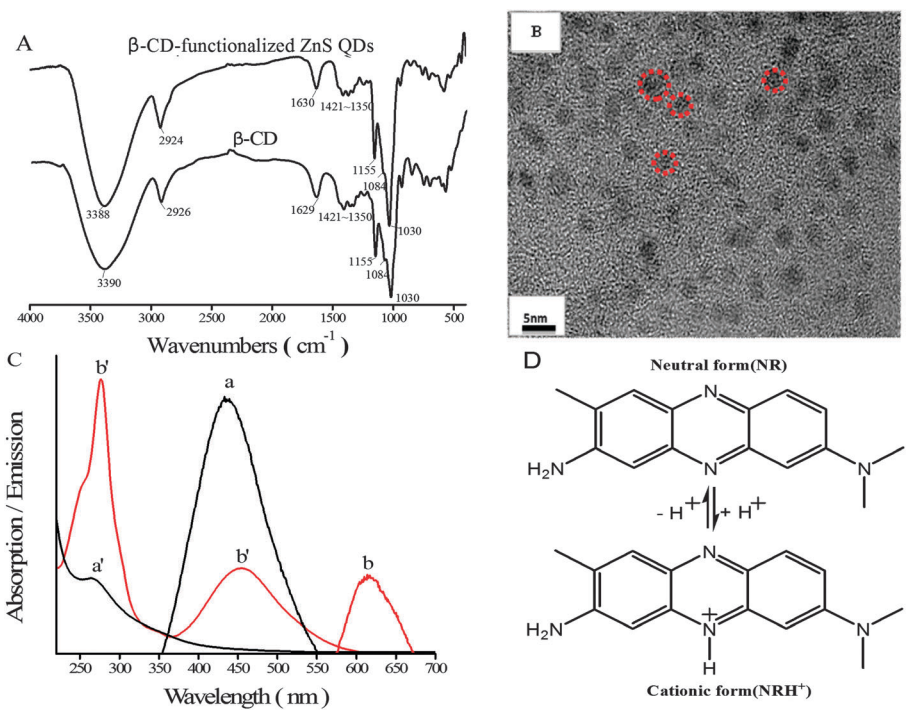

Fig. 1 (A) FTIR spectra of β-CD and β-CD-modified ZnS QDs. (B) The TEM image of β-CD modified ZnS QDs. (C) Spectral overlapping between β-CD modified ZnS QDs and NR. a and a′ lines represent the fluorescence emission band and the UV-vis absorption band of β-CD-modified ZnS QDs, respectively; b and b′ lines represent the fluorescence emission band and the UV-vis absorption band of NR, respectively. (D) The cationic form and the neutral form of neutral red (NR) in aqueous solution.

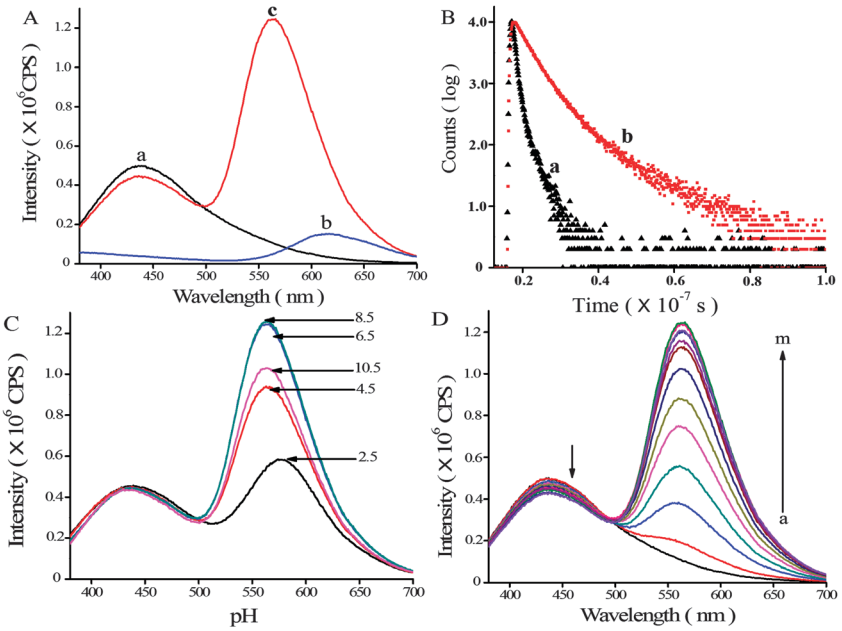

Fig. 2 (A) The fluorescence spectra of the β-CD-modified ZnS QDs (300 μM) and NR (1.8 μM) in pH 8.5 buffer solution (a, b), respectively; the fluorescence spectra of the mixture of NR and β-CD-modified ZnS QDs (1.8 μM + 300 μM) in pH 8.5 buffer solution (c), excited at λ = 300 nm. (B) The fluorescence decay curves of NR (1.8 μM) in the absence (a) and the presence (b) of β-CD-modified ZnS QDs (300 μM), monitored at λ = 564 nm. (C) The fluorescence intensities of the β-CD-QD–NR FRET fluorescence probe at pH 2.5, 4.5, 6.5, 8.5 and 10.5, respectively, excited at λ = 300 nm. (D) The fluorescence emission spectra of the β-CD-QD–NR FRET system at various concentrations of NR (from a to j, the concentrations of NR were 0, 0.2, 0.4, 0.6, 0.8, 1.0, 1.2, 1.4, 1.6, 1.8, 2.0, 2.2 and 2.4 μM, respectively), excited at λ = 300 nm.

of β-CD and β-CD-functionalized ZnS QDs. For the spectra of β-CD, the broad band at 3390 cm^{-1} and the band at 1629 cm^{-1} arise from the O–H stretching and asymmetric vibrations, respectively. The band at 2926 cm^{-1} corresponds to the asymmetric stretching vibration (ν_a) of the C–H bond, and the strong band at 1155 cm^{-1} and the bands at 1084 and 1030 cm^{-1} can be ascribed to the asymmetric glycosidic vibration ν_a(C–O–C) and the coupled stretching vibration ν(C–C and C–O), respectively. It can been seen from the FTIR spectra of the β-CD-functionalized ZnS QDs that the spectral features and peak positions of the main bands roughly resemble those of β-CD, which indicates that the β-CD has been successfully grafted onto the surfaces of the ZnS QDs.

Fig. 1B shows the high-resolution transmission electron microscopy image of the water-soluble β-CD-functionalized ZnS QDs. It can be seen from the image that the diameters of the particles range from 2 to 4 nm, and the sizes of the particles are virtually identical, indicating that the β-CD-functionalized ZnS QDs are monodispersed and uniform in water.

The UV-vis absorption and fluorescence emission spectra of the β-CD functionalized ZnS QDs are shown in Fig. 1C. The maximum absorption and emission bands of the β-CD functionalized ZnS QDs were at 270 nm and 435 nm, respectively, demonstrating that grafting the β-CD onto the QDs does not significantly influence the optical properties of the QDs.

Neutral red (NR) is a photoactive phenazine dye that generally exists in two molecular forms in aqueous solution, both an acidic and a neutral form[53] (see Fig. 1D). As shown in Fig. 1C, the UV-vis spectrum of NR has two absorption bands (the band at 278 nm can be attributed to the benzene ring, and the band at 454 nm arises from the conjugated three-ring system of the NR molecule). The fluorescence emission band of NR was at 614 nm when excited at λ = 300 nm. There was a remarkable overlapping between the fluorescence emission band of the QDs (donors) and the UV absorption band (454 nm) of the NR (acceptor), indicating that they would potentially provide an efficient fluorescence energy transfer from the QDs to the dye NR if the NR can enter the cavity of the β-CD on the surfaces of the QDs.

The quantum yield of the β-CD-functionalized ZnS QDs was determined to be 22.5%, which indicated that they can be used for determination purposes.[54]

3.2. Establishment of the β-CD-QD–NR fluorescence FRET probe

3.2.1. The β-CD-QD–NR FRET system. When the β-CD-functionalized ZnS QDs were mixed with the dye NR in basic buffer solution, FRET could be observed between them. As shown in Fig. 2A, the fluorescence emission intensities (at 435 nm) of the ZnS QDs slightly decreased, and a strong fluorescence emission band suited at approximately 564 nm appeared, which may be the blue-shifted band of NR. It is observed that the fluorescence emission band of the free NR was very weak (at 614 nm).

For a control, 3-mercaptopropionic acid (MPA)-capped ZnS QDs were prepared, and the optical properties of the mixture of MPA-capped ZnS QDs and NR were determined. The results showed that the FRET phenomenon cannot occur between these complexes (see Fig. S1, ESI†). The FRET between the

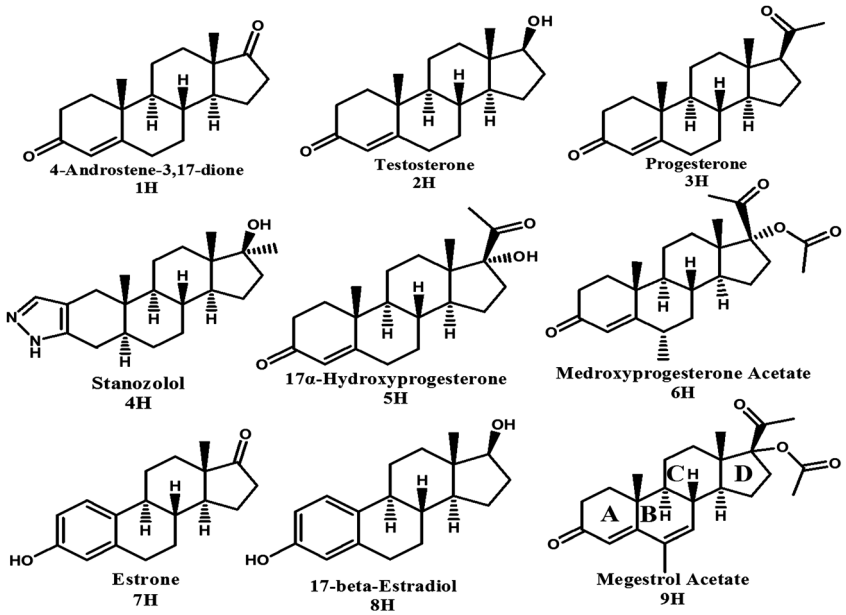

Fig. 3 The chemical structures of the nine steroid hormones.

β-CD-functionalized ZnS QDs and NR illustrated that the NR molecule entered the cavity of the β-CD on the surface of the ZnS QDs, decreasing the distance between these molecules. The blue shift of the fluorescence emission band for the NR probably originated from a conformational change after NR interacted with the β-CD and from alterations under the environmental conditions after NR entered the hydrophobic cavity.[53]

Fig. 2B shows the decay curves of NR before and after NR entered the cavity of the β-CD on the surface of ZnS QDs (monitored at λ = 564 nm), and the decay profiles were well fitted with a three-component exponential function, $I(t) = \alpha_1 \exp(-t/\tau_1) + \alpha_2 \exp(-t/\tau_2) + \alpha_3 \exp(-t/\tau_3)$.[55] The average fluorescence lifetimes of NR were calculated to be 3.62×10^{-11} and 1.15×10^{-9} s. It can be seen that the lifetime of NR has substantially increased after NR enters the cavity, which further supports the occurrence of FRET between β-CD-functionalized ZnS QDs and NR. As expected, the surface-anchored β-CD on ZnS QDs still retained their host capability of including molecular guests in their hydrophobic cavities.

3.2.2. The effects of pH on the properties of the probe. Fig. 2C shows the effects of pH (2.5, 4.5, 6.5, 8.5 and 10.5) on the fluorescence emission intensity of NR in the β-CD-QD–NR FRET probe system. It can be seen that the fluorescence intensities of NR were relatively low under acidic conditions (pH 2.5 and 4.5), and the intensities increased as the pH of the buffer solution was increased to 6.5 and 8.5. However, the intensity decreased when the pH reached 10.5. Conversely, the pH of the phosphate buffer solution has nearly no effect on the fluorescence intensities of β-CD-functionalized ZnS QDs. The NR existed in its neutral form under basic conditions (as shown in Fig. 1D), and the results indicated that the neutral form of NR was favoured to enter the cavity of the β-CD and form the FRET system. Thus, the optimal pH condition was selected as 8.5.

3.2.3. Optimization of the concentration of the NR in the probe. The fluorescence emission spectra of the β-CD-QD–NR FRET system at different concentrations of NR were measured in the buffer solution at pH 8.5 (see Fig. 2D). It can be seen that the fluorescence intensities of the ZnS QDs (at 435 nm) slightly decreased with increasing concentrations of NR, while those of NR (at 564 nm) significantly increased. When the concentration of NR increased to 1.8 μM (the concentration of the β-CD-functionalized ZnS QDs was 300 μM), the fluorescence intensity of the NR reached its maximum and did not change further by an additional increase in the concentration of NR. The β-CD-functionalized ZnS QD FRET system concentrations were thus set at 300 μM for β-CD-functionalized ZnS QDs and 1.8 μM for NR.

3.3. Response of the β-CD-QD–NR FRET fluorescence probe to steroid hormones

3.3.1. Specificity of the probe to megestrol acetate. The influence of nine steroid hormones, including 4-androstene-3,17-dione (1H), testosterone (2H), progesterone (3H), stanozolol (4H), 17α-hydroxy-progesterone (5H), medroxy-progesterone acetate (6H), estrone (7H), 17-beta-estradiol (8H) and megestrol acetate (9H) was analysed. Their structures are shown in Fig. 3.

The fluorescence intensity of the β-CD-QD–NR FRET probe has been investigated at three concentration levels (10, 60 and 180 μM), and the results are shown in Fig. 4. It can be seen that the fluorescence intensities of the probe (at 564 nm) were significantly quenched upon increasing the concentration of the megestrol acetate, while they were nearly unchanged when the concentrations of the other eight steroid hormones were lower than 60 μM. This result provided an opportunity for us to selectively determine the megestrol acetate at a lower concentration level. However, the fluorescence intensities of the probe can be obviously quenched by the other eight steroid hormones

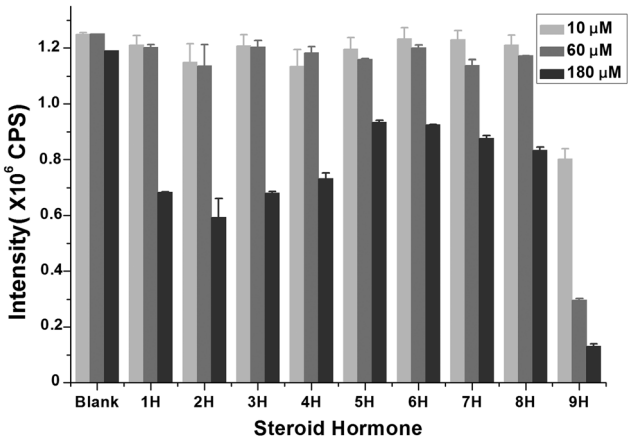

Fig. 4 The fluorescence intensities (at 564 nm) of the β-CD-QD–NR FRET fluorescence probe before and after interacting with various concentrations of nine steroid hormones, respectively, in the buffer solution (pH 8.5). The concentrations of the steroid hormones were 10, 60 and 180 μM, respectively, β-CD-modified ZnS QDs (300 μM), NR (1.8 μM), excited at λ = 300 nm. The results were the average of three repeats.

at high concentration levels (see Fig. 4, and Fig. S2, the ESI† shows the representative fluorescence quenching spectra of the probe by 5H), which may potentially be utilized to monitor the total content of the steroid hormones.

It was interesting to note that the megestrol acetate (9H) can obviously quench the fluorescence intensities of the QDs at 435 nm for the probe, and the other eight hormones (1H to 8H) have little effect on them at low concentration levels (10 and 60 μM). Conversely, these steroid hormones can cause the enhancement of the fluorescence emission bands for the QDs to various extents when the concentration of the other hormones reaches 180 μM (see Fig. S3, ESI†). This phenomenon and different fluorescence quenching behaviours of the nine hormones with respect to the probe have implied that the interaction mechanism between the megestrol acetate and the β-CD-QD–NR FRET probe was different from that for the other eight hormones.

3.3.2. Interaction mechanism of the probe and steroid hormones. To explore the fluorescence quenching mechanism of the β-CD-QD–NR FRET probe, the average fluorescence lifetimes of NR (τ) for the probe after interacting with the steroid hormones have been determined individually. The results indicated that the lifetime of the NR in the probe for 9H was 1.08×10^{-9} s, which was similar to that of the NR (1.15×10^{-9} s) prior to interacting with 9H (see Fig. S4A, ESI†). This lifetime was much greater than the fluorescence lifetime of NR (3.62×10^{-11} s) in the free state (in buffer solution). This result illustrated that the 9H did not displace the NR from the cavity of the β-CD on the surface of the ZnS QDs after interacting with the probe and that the fluorescence quenching of the probe may originate from the combination of 9H and the NR in the cavity of the β-CD, forming complexes that have no fluorescence.

After interacting with the other eight steroid hormones (1H to 8H, 180 μM), the fluorescence lifetimes of NR ($\tau \times 10^{-11}$ s) were 7.24, 8.99, 7.81, 8.14, 13.0, 6.84, 9.23 and 8.62 (Fig. S4B, ESI† shows the representative decay curves of NR for the probe before and after interacting with the 5H), and these lifetimes were significantly lower than that of the NR (1.15×10^{-9} s) prior to interaction with the steroid hormones and much closer to that of the NR in the free state. It has been inferred that the NR molecule may be partly removed from the cavity of the β-CD by these steroid hormones at higher concentration levels, which leads to the interruption of the FRET process and causes the reduction of the fluorescence emission intensities at 564 nm and the fluorescence enhancement of the QDs (at 435 nm) (see Fig. S2 and S3, ESI†).

For the confirmation of the above suppositions, control experiments have been performed (see Fig. 5A). The fluorescence spectra of the NR solution and its mixture with a β-CD solution were collected, and the results showed that the fluorescence emission intensity of the mixture of NR and β-CD was obviously

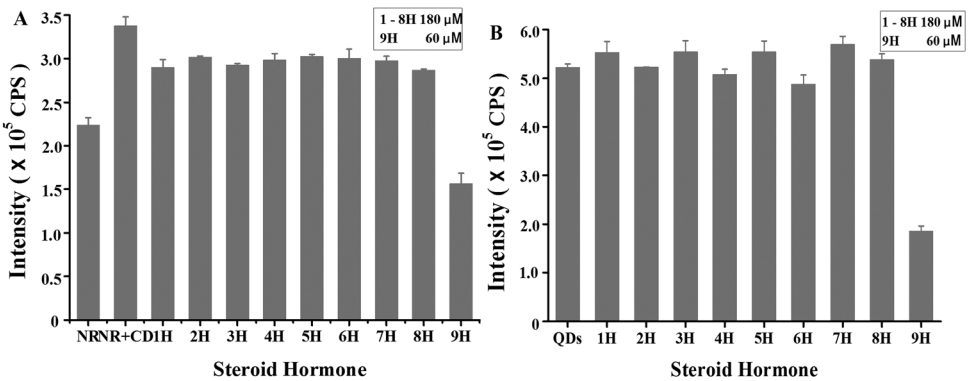

Fig. 5 (A) Control experiments for the interaction of NR and steroid hormones. The NR column represents the fluorescence intensity of individual NR (1.8 μM); the NR + CD column represents the fluorescence intensity of NR (1.8 μM) after the addition of the β-CD (300 μM) solution; 1–9H columns represent the fluorescence intensity of NR after mixing with the β-CD solution and the nine steroid hormones (megestrol acetate (60 μM) and other steroid hormones (180 μM)), respectively. All fluorescence spectra were monitored at λ = 564 nm and excited at λ = 300 nm. (B) Control experiments for the interaction of β-CD-modified ZnS QDs and steroid hormones. QDs column represents the fluorescence intensity (at 435 nm) of the β-CD-modified ZnS QDs (300 μM), 1–9H columns represent the fluorescence intensity (at 435 nm) of β-CD-modified ZnS QDs after the addition of various steroid hormones (1–9H) (megestrol acetate (60 μM) and other steroid hormones (180 μM)), respectively, excited at λ = 300 nm. The results were the average of three repeats.

higher than that of the free NR solution. This implied that the NR molecule entered the cavity of the β-CD. When the steroid hormones (1H–8H) were added to the mixture solution individually, the fluorescence intensities of the mixture solution decreased, but they were still higher than that of the free NR. This result suggests that the NR molecule is partly displaced by the steroid hormones. However, after interaction with the steroid hormone 9H, the fluorescence intensity of the mixture was significantly decreased and was lower than those of the mixture and the free NR solution, which illustrated that 9H combined with the NR molecule and formed a complex. The results of the control experiments were similar to those of the interactions between the β-CD-QD–NR FRET probe and the steroid hormones, and it has been verified that above suppositions are rational.

Similarly, the influence of the steroid hormones on the fluorescence intensities of the β-CD functionalized QDs has also been investigated. The results showed that the megestrol acetate (9H) can significantly quench the fluorescence of the β-CD-functionalized QDs (at 435 nm), while the other eight steroid hormones have nearly no effect on the fluorescence intensities of the QDs (see Fig. 5B). This control experiment illustrated that the fluorescence quenching of the β-CD-QD–NR FRET probe (at 435 nm) may originate from the combination of 9H with the QDs. Therefore, it can be concluded that the megestrol acetate can form a complex with the NR molecule and combine with the ZnS QDs in the probe, which interrupts the FRET process and induces fluorescence quenching of the probe.

The structure of megestrol acetate was different from that of the other eight steroid hormones (see Fig. 3). For megestrol acetate, the carbonyl group connected to ring A was conjugated with the two double bonds of rings A and B, forming a larger conjugated system. Therefore, the oxygen atom of the carbonyl group would carry more negative charge and would enhance its hydrogen bonding capability with the amino group of the NR molecule or combine with the Zn^{2+} on the surface of the QDs. For the other steroid hormones, the carbonyl group of ring A was only conjugated with one double bond in ring A (1H, 2H, 3H, 5H and 6H), the hydroxyl group on ring A was conjugated with the benzene ring (7H and 8H), or an imidazole ring connected to ring A (4H). These functional groups of the steroid hormones do not have enough electronegativity to combine with the QDs or NR molecule, while they can enter the cavity of the β-CD and replace the NR molecule at high concentration levels.

Major ions and trace metals are usually present in aquatic systems.[56] In order to observe the influences of these ions on the determination of megestrol acetate, the effects for 10 kinds of common ions (Ca^{2+}, Cd^{2+}, Mn^{2+}, Co^{2+}, Mg^{2+}, Na^{+}, K^{+}, Fe^{3+}, Fe^{2+} and Cu^{2+}) on the β-CD-QD–NR FRET fluorescence probe have been investigated (see Fig. S5, ESI†), individually. As shown in Fig. S5 (ESI†), the fluorescence intensities of the probe (at 564 nm) were nearly unchanged upon adding various ions, which demonstrated that the common coexisting ions in water did not interfere with the results for the determination of the megestrol acetate.

3.4. Application of the β-CD-QD–NR FRET fluorescence probe for the determination of megestrol acetate in river water samples

3.4.1. Relationship of the fluorescence intensities for the probe with the concentrations of megestrol acetate. As discussed above, the β-CD-QD–NR FRET fluorescence probe was sensitive and specific to megestrol acetate at a lower concentration level, and therefore, the determination method for megestrol acetate concentration described herein has been investigated and developed.

Fig. 6A shows the fluorescence quenching spectra of the probe with various concentrations of megestrol acetate in the range of 0–60 μM. It can be seen that the fluorescence intensities of the probe have been gradually decreased upon increasing the concentrations of the megestrol acetate, and their relationship has been calculated based on the Stern–Volmer equation,[57] as follows:

$$\frac{I_0}{I} = 1 + k_Q\tau_0[Q] = 1 + K_{SV}[Q] \quad (1)$$

where I_0 and I represent the fluorescence intensities of the probe in the absence and presence of megestrol acetate, $[Q]$ is the concentration of the megestrol acetate and τ_0 is the average lifetime of the probe in the absence of megestrol acetate. The quantities k_Q and K_{sv} are the quenching rate constant and Stern–Volmer quenching constants, respectively.

As shown in Fig. 6B, the curve for the fluorescence quenching fractions of the probe *versus* the concentrations of megestrol acetate presents satisfactory linearity in the concentration ranging from 0.25 μM to 60 μM. The linear regression equation was $y = 0.0514x - 0.00124$ with a regression coefficient (r) of 0.999, which indicated that the β-CD-QD–NR FRET fluorescence probe can be utilized with confidence to determine the megestrol acetate concentration. The limit of detection (LOD) for the probe was evaluated using $3\sigma/S$ and was found to be 0.0083 μM, where σ is the standard deviation of the blank signal, and S is the slope of the linear calibration plot.[58]

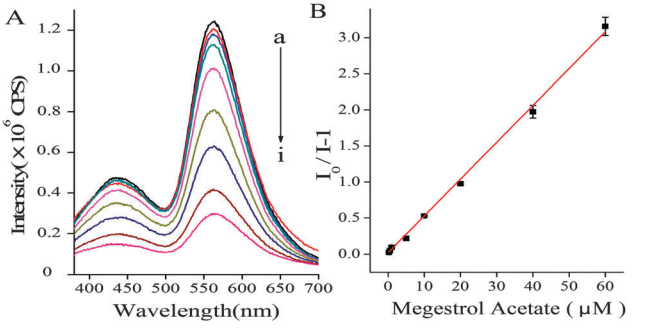

Fig. 6 (A) The fluorescence quenching spectra of the β-CD-QD–NR FRET fluorescence probe induced by various concentrations of megestrol acetate (from a to i: 0, 0.25, 0.5, 1.0, 5.0, 10, 20, 40 and 60 μM) in buffer solution (pH 8.5), β-CD-modified ZnS QDs (300 μM), NR (1.8 μM), excited at λ = 300 nm. (B) The Stern–Volmer plot for the fluorescence quenching fractions (at λ = 564 nm) of the probe *versus* the concentrations of megestrol acetate. The results were the average of three repeats.

The quenching rate constant k_Q of the probe (NR) was calculated to be 4.47×10^{13} L mol^{-1} s^{-1} ($\tau_0 = 1.15 \times 10^{-9}$ s) according to the above Stern–Volmer curve, which was approximately three orders of magnitude higher than the limiting diffusion constant K_{dif} of the biomolecule ($K_{dif} = 2.0 \times 10^{10}$ L mol^{-1} s^{-1}).[59,60] The results illustrated that a specific interaction between the probe and megestrol acetate has occurred, and their fluorescence quenching mainly arose from static quenching by forming a complex[59,61] between the probe and megestrol acetate.

The binding number (n) of megestrol acetate on the probe was calculated according to the following eqn (2), where K_A is the binding constant. The results showed that $n = 0.85$, which indicated that the ratio of probe and megestrol acetate in the complex was approximately 1 : 1.

$$\lg\left(\frac{I_0 - I}{I}\right) = \lg K_A + n \log[Q] \quad (2)$$

In this case, the binding constant (K_A) of the complex can be obtained from the slope of the curve based on the following eqn (3), and the calculated apparent K_A was 9.52×10^4 L mol^{-1}. The large value of K_A illustrated that the megestrol acetate molecule has a high ability to bind with the probe, inducing its significant fluorescence quenching, which further supported the mechanism deduced in Section 3.3.2.

$$\frac{I_0}{I_0 - I} = 1 + K_A^{-1}[Q]^{-1} \quad (3)$$

3.4.2. Spiking recoveries of megestrol acetate in river water. The content of the steroid hormones in river water was generally very low, so sample pretreatment procedures for purification and enrichment were needed. Usually, the enrichment factor for HPLC and MS methods was approximately 1000.[41,48] Different spiking levels of megestrol acetate with concentrations ranging from 0.001 μM to 10 μM in the river water samples were performed, and the samples were then enriched and purified using SPE procedures.[41,48] Thereafter, the concentrations of the residues were determined using the developed β-CD-QD–NR FRET fluorescence probe, and the results are summarized in Table 1. It can be seen from the data in Table 1 that the average recoveries of megestrol acetate ranged from 97 to 110%, with relative standard deviations (RSD) below 15%, which satisfied the demands of residue analysis.[62] Considering the enrichment factor, theoretically, the limit of detection (LOD) for the established method was 0.083 nM (the enrichment factor was 100). It can be noted from the data shown in Table 1 that the limit of quantification (LOQ) can reach 1.0 nmol, and the standard deviations would become very large upon decreasing the spiking levels, which cannot guarantee the accuracy of the determination results. In this case, the LOD and LOQ of the developed method were nearly equal to those of previous reports for HPLC-MS[49] or GC-MS[48] methods, and were significantly lower than those of HPLC approaches.[63] As the data shown in Table 1, the satisified spiking recoveries and RSD have been obtained in the concentration range between 1.0 nM and 10 μM, which can be considered as the detection range of the megestrol acetate for the developed method, and was much better than those of previous reports.[49,63] The results illustrated that the method is sensitive and can be utilized for the rapid determination of megestrol acetate in river water samples.

Table 1 Analytical results for the detection of megestrol acetate levels in river sample (n = 5)

Content of megestrol acetate (μM)	Recovery (%)	RSD (%)
0.001	108.66	9.23
0.01	109.62	13.34
0.1	96.64	6.59
1.0	100.52	4.14
10	100.14	5.44

4. Conclusions

A novel beta-cyclodextrin functionalized ZnS quantum dot–neutral red (NR) fluorescence resonance energy transfer probe for the determination of megestrol acetate concentrations in river water samples has been developed. The synthesis of the water-soluble and low toxicity beta-cyclodextrin-functionalized ZnS quantum dots was first reported in this paper. The dye neutral red in its neutral form can enter the cavity of beta-cyclodextrin anchored onto the surface of ZnS quantum dots, forming an efficient fluorescence resonance energy transfer fluorescence system. The interaction mechanisms of the obtained probe with nine types of steroid hormones have been investigated, and the results showed that megestrol acetate induced the fluorescence quenching of the fluorescence resonance energy transfer probe by forming complex, which was different from the mechanisms for other steroid hormones. The fluorescence resonance energy transfer fluorescence probe was specific for megestrol acetate at low concentration levels, and the developed method was specific, rapid and sensitive. This methodology can determine the megestrol acetate concentrations in river water samples at the nanomolar level when combined with the reported sample pretreatment procedures and is equivalent to high performance liquid chromatography or mass spectrometry techniques.

Acknowledgements

This work was financially supported by the national science and technology support program (2012BAK26B04).

Notes and references

1 J. P. Yuan, W. W. Guo, X. R. Yang and E. Wang, *Anal. Chem.*, 2009, **81**, 362–368.
2 J. Y. Kim, O. Voznyy, D. Zhitomirsky and E. H. Sargent, *Adv. Mater.*, 2013, **25**, 4986–5010.
3 P. Wu, T. Zhao, S. L. Wang and X. D. Hou, *Nanoscale*, 2014, **6**, 43–64.

4 K. E. Knowles, D. B. Tice, E. A. McArthur, G. C. Solomon and E. A. Weiss, *J. Am. Chem. Soc.*, 2010, **132**, 1041–1050.
5 M. Li, Q. Y. Wang, X. D. Shi, L. A. Hornak and N. Q. Wu, *Anal. Chem.*, 2011, **83**, 7061–7065.
6 H. B. Li, Y. Zhang, X. Q. Wang, D. J. Xiong and Y. Q. Bai, *Mater. Lett.*, 2007, **61**, 1474–1477.
7 S. Shiosaki, T. Nobori, T. Mori, R. Toita, Y. Nakamura, C. W. Kim, T. Yamamoto, T. Niidome and Y. Katayama, *Chem. Commun.*, 2013, **49**, 5592–5594.
8 D. Zhao, J. T. Li, T. M. Yang and Z. K. He, *Biosens. Bioelectron.*, 2014, **52**, 29–35.
9 Y. Z. Wu, K. Eisele, M. Doroshenko, G. Algara-Siller, U. Kaiser, K. Koynov and T. Weil, *Small*, 2012, **8**, 3465–3475.
10 C. W. Peng, Q. Tian, G. F. Yang, M. Fang, Z. L. Zhang, J. Peng, Y. Li and D. W. Pang, *Biomaterials*, 2012, **33**, 5742–5752.
11 J. Gong, X. Q. An and X. J. Yan, *New J. Chem.*, 2014, **38**, 1376–1379.
12 Y. F. Chen and Z. Rosenzweig, *Anal. Chem.*, 2002, **74**, 5132–5138.
13 M. C. Brelle, J. Z. Zhang, L. Nguyen and R. K. Mehra, *J. Phys. Chem. A*, 1999, **103**, 10194–10201.
14 H. Zhang, Z. Zhou, B. Yang and M. Y. Gao, *J. Phys. Chem. B*, 2003, **107**, 8–13.
15 R. Kho, C. L. Torres-Martinez and R. K. Mehra, *J. Colloid Interface Sci.*, 2000, **227**, 561–566.
16 H. Meng, J. Y. Chen, L. Mi, P. N. Wang, M. Y. Ge, Y. Yue and N. Dai, *JBIC, J. Biol. Inorg. Chem.*, 2011, **16**, 117–123.
17 S. F. Xu, H. Z. Lu, J. H. Li, X. L. Song, A. X. Wang, L. X. Chen and S. B. Han, *ACS Appl. Mater. Interfaces*, 2013, **5**, 8146–8154.
18 J. B. Delehanty, C. E. Bradburne, K. Susumu, K. Boeneman, B. C. Mei, D. Farrell, J. B. Blanco-Canosa, P. E. Dawson, H. Mattoussi and I. L. Medintz, *J. Am. Chem. Soc.*, 2011, **133**, 10482–10489.
19 S. Su, J. W. Fan, B. Xue, L. H. Yuwen, X. F. Liu, D. Pan, C. H. Fan and L. H. Wang, *ACS Appl. Mater. Interfaces*, 2014, **6**, 1152–1157.
20 M. Algarra, B. B. Campos, F. R. Aguiar, J. E. Rodriguez-Borges and J. da Silva, *Mater. Sci. Eng., C*, 2012, **32**, 799–803.
21 J. M. Li, M. X. Zhao, H. Su, Y. Y. Wang, C. P. Tan, L. N. Ji and Z. W. Mao, *Biomaterials*, 2011, **32**, 7978–7987.
22 X. Wang, X. H. Lou, Y. Wang, Q. C. Guo, Z. Fang, X. H. Zhong, H. J. Mao, Q. H. Jin, L. Wu, H. Zhao and J. L. Zhao, *Biosens. Bioelectron.*, 2010, **25**, 1934–1940.
23 H. B. Li and C. P. Han, *Chem. Mater.*, 2008, **20**, 6053–6059.
24 Q. A. Jiang, H. Y. Zhang and Y. Liu, *Chin. Sci. Bull.*, 2010, **55**, 2835–2839.
25 I. Shown, M. Ujihara and T. Imae, *J. Colloid Interface Sci.*, 2010, **352**, 232–237.
26 P. Liu, X. L. Sun, W. He, R. Jiang, P. G. Wang, Y. Zhao and S. Y. Zhang, *J. Sep. Sci.*, 2009, **32**, 125–134.
27 L. Wang, S. P. Liu, J. J. Peng and Y. Q. He, *Sci. China: Chem.*, 2010, **53**, 1358–1365.
28 C. P. Han and H. B. Li, *Small*, 2008, **4**, 1344–1350.
29 R. Freeman, T. Finder, L. Bahshi and I. Willner, *Nano Lett.*, 2009, **9**, 2073–2076.
30 X. Z. Ai, L. Niu, Y. Y. Li, F. P. Yang and X. G. Su, *Talanta*, 2012, **99**, 409–414.
31 K. Palaniappan, S. A. Hackney and J. Liu, *Chem. Commun.*, 2004, 2704–2705.
32 W. R. Algar and U. J. Krull, *Anal. Bioanal. Chem.*, 2008, **391**, 1609–1618.
33 A. M. Dennis, W. J. Rhee, D. Sotto, S. N. Dublin and G. Bao, *ACS Nano*, 2012, **6**, 2917–2924.
34 D. M. Willard, L. L. Carillo, J. Jung and A. Van Orden, *Nano Lett.*, 2001, **1**, 469–474.
35 J. E. Ghadiali, B. E. Cohen and M. M. Stevens, *ACS Nano*, 2010, **4**, 4915–4919.
36 C. W. Chi, Y. H. Lao, Y. S. Li and L. C. Chen, *Biosens. Bioelectron.*, 2011, **26**, 3346–3352.
37 Y. Wu, Y. P. Ho, Y. C. Mao, X. M. Wang, B. Yu, K. W. Leong and L. J. Lee, *Mol. Pharmaceutics*, 2011, **8**, 1662–1668.
38 H. F. Dong, W. C. Gao, F. Yan, H. X. Ji and H. X. Ju, *Anal. Chem.*, 2010, **82**, 5511–5517.
39 S. Hartmann, M. Lacorn and H. Steinhart, *Food Chem.*, 1998, **62**, 7–20.
40 M. J. L. de Alda, S. Diaz-Cruz, M. Petrovic and D. Barcelo, *J. Chromatogr. A*, 2003, **1000**, 503–526.
41 Y. F. Hu, M. Zhang, C. L. Tong, J. M. Wu and W. P. Liu, *J. Sep. Sci.*, 2013, **36**, 3321–3329.
42 Y. B. Fan, Y. M. Yin, W. B. Jiang, Y. P. Chen, J. W. Yang, J. Wu and M. X. Xie, *Food Chem.*, 2014, **142**, 170–177.
43 C. M. Lu, M. T. Wang, J. Mu, D. C. Han, Y. P. Bai and H. Q. Zhang, *Food Chem.*, 2013, **141**, 1796–1806.
44 Y. F. Hu, M. Zhang, C. L. Tong, J. M. Wu and W. P. Liu, *J. Sep. Sci.*, 2013, **36**, 3321–3329.
45 N. Swart and E. Pool, *J. Immunoassay Immunochem.*, 2007, **28**, 395–408.
46 F. Long, H. C. Shi and H. C. Wang, *RSC Adv.*, 2014, **4**, 2935–2941.
47 M. X. Zhao, Q. Xia, X. D. Feng, X. H. Zhu, Z. W. Mao, L. N. Ji and K. Wang, *Biomaterials*, 2010, **31**, 4401–4408.
48 M. Miclean, L. Senila, C. Roman, A. Gog, E. Levei and I. Groza, *Rev. Chim.*, 2010, **61**, 615–618.
49 M. J. L. de Alda and D. Barcelo, *J. Chromatogr. A*, 2000, **892**, 391–406.
50 A. Rogalski and K. Chrzanowski, *Opto-Electron. Rev.*, 2002, **2**, 111–136.
51 D. S. Hobbs and B. D. MacLeod, in *Window and Dome Technologies and Materials IX*, ed. R. W. Tustison, Spie-Int Soc Optical Engineering, Bellingham, 2005, vol. 5786, pp. 349–364.
52 M. A. Pickering, R. L. Taylor and D. T. Moore, *Appl. Opt.*, 1986, **25**, 3364–3372.
53 J. Mohanty, A. C. Bhasikuttan, W. M. Nau and H. Pal, *J. Phys. Chem. B*, 2006, **110**, 5132–5138.
54 X. Y. Cao, F. Shen, M. W. Zhang, J. X. Bie, X. Liu, Y. L. Luo, J. J. Guo and C. Y. Sun, *RSC Adv.*, 2014, **4**, 16597–16606.

55 U. Noomnarm and R. M. Clegg, *Photosynth. Res.*, 2009, **101**, 181–194.
56 J. P. Kim and K. A. Hunter, *Mar. Freshwater Res.*, 1997, **48**, 257–266.
57 A. Papadopoulou, R. J. Green and R. A. Frazier, *J. Agric. Food Chem.*, 2005, **53**, 158–163.
58 G. C. Tang, L. P. Du and X. G. Su, *Food Chem.*, 2013, **141**, 4060–4065.
59 J. R. Akowicz, *Principles of Fluorescence Spectroscopy*, Kluwer Academic/Plenum Publishers, New York, 2nd edn, 1999.
60 W. R. Ware, *J. Chem. Phys.*, 1962, **37**, 923–924.
61 C. Qin, M. X. Xie and Y. Liu, *Biomacromolecules*, 2007, **8**, 2182–2189.
62 C. C. Chang and S. D. Huang, *Anal. Chim. Acta*, 2010, **662**, 39–43.
63 C. Almeida and J. M. F. Nogueira, *J. Pharm. Biomed. Anal.*, 2006, **41**, 1303–1311.